Computers in Biology and Medicine 37 (2007) 1292 – 1302

Computers in Biology and Medicine

www.intl.elsevierhealth.com/journals/cobm

A novel active contour model for fully automated segmentation of intravascular ultrasound images: In vivo validation in human coronary arteries☆

George D. Giannoglou[a,*], Yiannis S. Chatzizisis[a], Vassilis Koutkias[b], Ioannis Kompatsiaris[c], Maria Papadogiorgaki[c], Vasileios Mezaris[c], Eirini Parissi[c], Panagiotis Diamantopoulos[d], Michael G. Strintzis[c], Nicos Maglaveras[b], George E. Parcharidis[a], George E. Louridas[a]

[a] *Cardiovascular Engineering and Atherosclerosis Laboratory, 1st Cardiology Department, AHEPA University Hospital, Aristotle University Medical School, Thessaloniki, Greece*

[b] *Laboratory of Medical Informatics, Aristotle University Medical School, Thessaloniki, Greece*

[c] *Informatics and Telematics Institute, Center for Research and Technology-Hellas, Thessaloniki, Greece*

[d] *Department of Engineering and Design, University of Sussex, Sussex, UK*

Received 13 October 2005; received in revised form 28 November 2006; accepted 4 December 2006

Abstract

The detection of lumen and media-adventitia borders in intravascular ultrasound (IVUS) images constitutes a necessary step for the quantitative assessment of atherosclerotic lesions. To date, most of the segmentation methods reported are either manual, or semi-automated, requiring user interaction at some extent, which increases the analysis time and detection errors. In this work, a fully automated approach for lumen and media-adventitia border detection is presented based on an active contour model, the initialization of which is performed via an analysis mechanism that takes advantage of the inherent morphologic characteristics of IVUS images. The in vivo validation of the proposed model in human coronary arteries revealed that it is a feasible approach, enabling accurate and rapid segmentation of multiple IVUS images.

Keywords: Intravascular ultrasound (IVUS); Segmentation; Active contour models; Coronary arteries

1. Introduction

Coronary angiography is the gold-standard method for imaging and diagnosis of coronary heart disease. However, it is restricted by its inability to quantify plaque burden beyond the luminal silhouette created by the angiographic contrast. In the recent years, intravascular ultrasound (IVUS) has been proven superior in the imaging of coronary atherosclerosis [1]. IVUS is a catheter-based technique that provides two-dimensional (2D) cross-sectional images of coronary artery and, therefore, accurate information about the arterial morphometry (i.e. lumen, vessel and plaque area) and morphology. However, 2D IVUS images are limited in providing reliable information about the extent of atherosclerosis due to their tomographic nature. Aiming to overcome this limitation, several three-dimensional (3D) reconstructions approaches have been developed based on either linear stacking of adjacent IVUS images, resulting in straight 3D reconstruction, or spatially correct localization of adjacent IVUS images along the vessel course, resulting in anatomically realistic 3D reconstructions [2–6].

The first and most critical step for the 3D reconstruction of coronary arteries, regardless of the reconstruction approach, is the segmentation of the IVUS images, i.e. the detection of the lumen-wall and media-adventitia borders (contours) (Fig. 1). Segmentation can be done either manually, which is a quite

☆ *Funding sources*: This work was granted by the Greek State Scholarships Foundation and the Aristotle University of Thessaloniki Research Committee.

* Corresponding author. Cardiovascular Engineering and Atherosclerosis Laboratory, 1st Cardiology Department, AHEPA University Hospital, Aristotle University Medical School, 1 St. Kyriakidi Street, 54636, Thessaloniki, Greece. Tel./fax: +30 2310 994837.

E-mail address: yan@med.auth.gr (G.D. Giannoglou).

0010-4825/$ - see front matter © 2007 Elsevier Ltd. All rights reserved.
doi:10.1016/j.compbiomed.2006.12.003

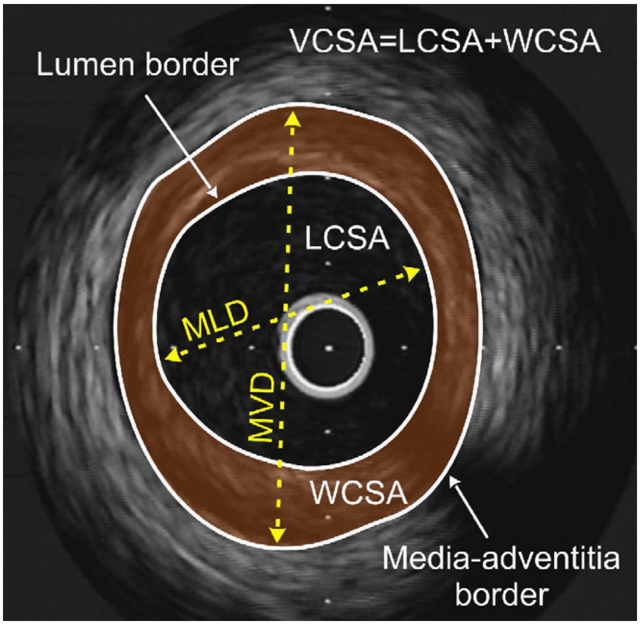

Fig. 1. A typical IVUS image with the lumen and media-adventitia borders demarcated (LCSA, lumen cross-sectional area; VCSA, vessel cross-sectional area; WCSA, wall cross-sectional area; MLD, maximum lumen diameter; MVD, maximum vessel diameter).

laborious and time-consuming process, subject to high inter- and intra-user variability, or via computer-aided techniques. Several IVUS segmentation approaches have been proposed so far, including texture analysis [7], active contours [8], knowledge-based graph searching [9], minimum cost algorithms [10], and region growing [11]. Among them, the active contour model and its variations showed remarkable feasibility and accuracy [12–14]. However, some of these algorithms require manual contour initialization, thereby increasing the user interaction, and concomitantly the uncertainty of the segmentation. In addition, although these algorithms were extensively validated in vitro, their in vivo applicability and reliability still remain unclear.

In this study, we present a fully automated approach for segmentation of IVUS images based on a variation of an active contour model, and, also, validate this approach in vivo in human coronary arteries. Considering an IVUS image sequence, the initialization of the lumen-wall and media-adventia contours in each image is performed automatically using an initialization algorithm, and the initial contours extracted constitute the input to the active contour model, which then deforms the contours appropriately, identifying their correct location on the IVUS frame. The in vivo evaluation of the proposed approach showed that our technique is capable of reliably and rapidly segmenting IVUS images, without requiring any additional user interaction.

2. Methods

2.1. Theoretical background

Active contour models, also known as snakes, were originally presented as a regularization step in edge detection algorithms [15–17]. A snake is an ordered set of points (called snaxels), constituting an energy-minimizing parametric closed curve guided by external forces, which has to be initially defined on the image plane. Specifically, the aim is to minimize an energy functional E_{snake}, defined as

$$E_{\text{snake}} = E_{\text{int}} + E_{\text{ext}}, \tag{1}$$

where E_{int} and E_{ext} are the internal energy formed by the snake configuration and the external energy formed by external forces affecting the snake, respectively. In this context, the initially defined contour deforms appropriately, in order to minimize the abovementioned energy functional.

Although several active contour models have been presented in the literature, exhibiting remarkable results in various application domains, one of their major drawbacks is the requirement for manual initialization of the active contours. In this study, we developed an automated mechanism for active contour initialization based on the analysis of inherent characteristics of IVUS images. This mechanism was incorporated in a variant active contour model that was constructed for efficient IVUS images segmentation. The entire segmentation model developed is presented in detail in the following.

2.2. IVUS images acquisition and pre-processing

The IVUS images acquisition process is summarized in Fig. 2 [18]. The IVUS procedures were performed with a mechanical imaging system (ClearView, Boston Scientific, Natick, MA, USA) and a 2.6F sheath-based catheter, incorporating a 40 MHz single-element transducer rotating at 1800 rpm and yielding 30 images/s (Atlantis SR Pro, Boston Scientific, Natick, MA, USA). A motorized pullback device was used to withdraw the catheter at a constant speed of 0.5 mm/s. The ultrasound data, along with the simultaneous ECG, was recorded in a 0.5 in S-VHS videotape. The S-VHS data was digitized at 512×512 pixels with 8-bit grey scale at a rate of 7.5 images/s, and the end-diastolic images were selected (peak of R-wave on ECG).

Then, the IVUS images were segmented according to the framework schematically presented in Fig. 3. The first step of the procedure involved the image pre-processing, in order to prepare appropriate versions of the images and increase the detection efficiency. From each IVUS image, a 340×340 pixels sub-image was extracted, including the region of interest and the transducer of the catheter at the center of the image. To facilitate efficient pre-processing in the radial and tangential direction, the sub-image was transformed to a polar coordinate image, where columns and rows corresponded to angle and distance from the center of the catheter, respectively. The polar coordinate image, denoted as $I(r, \theta)$, was used for the remainder of the pre-processing and contour initialization. In addition, the catheter induced artifacts were removed. As already mentioned, IVUS images include not only tissue and blood regions, but also the transducer of the catheter; the latter defines a dead zone of radius equal to that of the transducer, where no useful

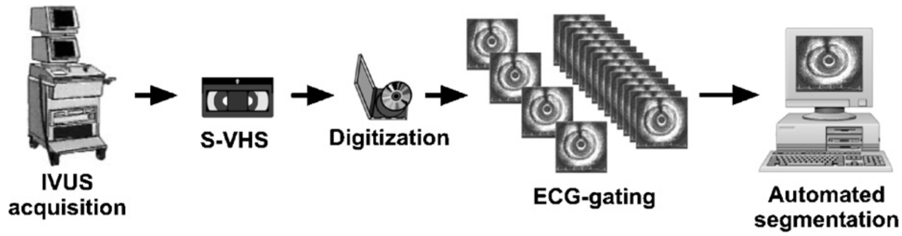

Fig. 2. Schematic presentation of IVUS images acquisition process.

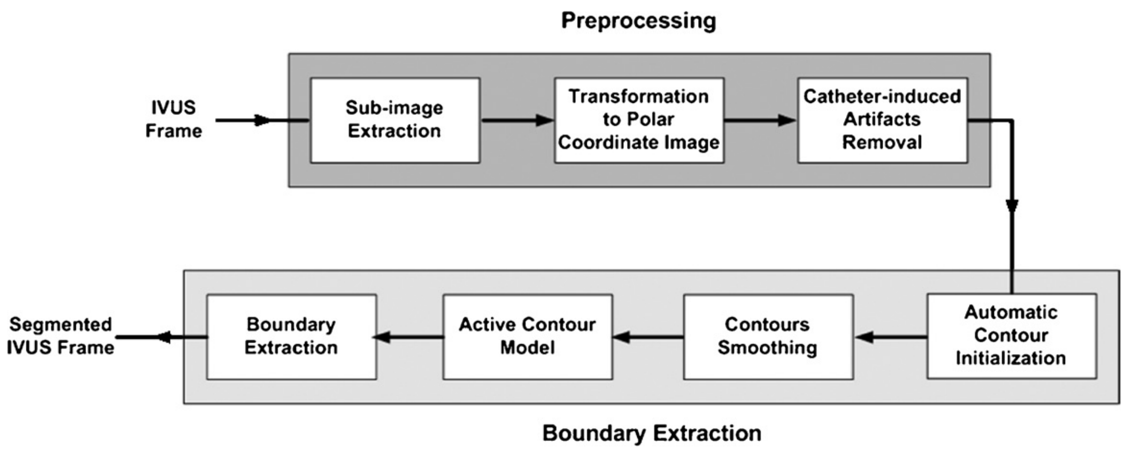

Fig. 3. The proposed approach for the automated segmentation of IVUS images.

information is contained (Fig. 1). Knowing the diameter D of the transducer, these catheter-induced artifacts were easily removed by setting $I(r,\theta)=0$ for $r<D/2+e$, with e being a small constant.

2.3. Automated contour initialization

Objective of the contour initialization procedure was the detection of pixels that are likely to belong to the lumen and media-adventitia borders. Two discrete initialization steps were defined to this end, each used for the initialization of the respective border [19].

At the first initialization step, intensity information was used for detecting in $I(r,\theta)$ artifacts marking the border between the lumen and wall structures. More specifically, the lumen border was initialized as the set of pixels $c_{\text{int}}=\{\mathbf{p}_{\text{int}}=[\rho,\theta]\}$, which satisfy the following condition:

$$I(\rho,\theta)>T \quad \text{and} \quad I(r,\theta)<T,\quad \forall r<\rho, \tag{2}$$

where T is a constant, the value of which was set experimentally. This procedure essentially took into account high-frequency details of $I(r,\theta)$ in the radial direction to localize the respective border.

As opposed to the first initialization step, which relied on exploiting high-frequency image information, in the second step low-frequency information was taken into account. The motivation behind this choice lies in the observation that in the IVUS image the adventitia is represented by a thick echodense ring which corresponds to a thick bright curve in polar coordinates in contrast to the echolucent lumen and intima/media structures. Thus, performing low-pass filtering to suppress high-frequency details corresponding to the latter, and, subsequently, considering only the remaining lower-frequency information is a justified choice for facilitating the correct localization of the media-adventitia border. More specifically, the media-adventitia border was initialized as the set of pixels $c_{\text{ext}}=\{p_{\text{ext}}=[\mu,\theta]\}$, for which

$$I_{\text{ext}}(\mu,\theta)=\max_{r>\rho}\{I_{\text{ext}}(r,\theta)\}, \tag{3}$$

where $[\rho,\theta]$ are the points of the initial internal contour and I_{ext} is obtained from I by means of low-pass filtering of I in the radial and tangential directions to suppress higher-frequency details corresponding to the internal contour. To this end, filters $H(z)$, $H(z^2)$, $H(z^4)$ and $H(z^8)$ were applied row-wise and column-wise to image I, where

$$H(z)=\tfrac{1}{2}(1+z^{-1}). \tag{4}$$

Contour initialization was completed by smoothing the initial contours c_{int}, c_{ext}, so that they can better approximate the true luminal and media-adventitia borders, which are smooth, continuous functions of θ. This was performed by means of contour low-pass filtering in the tangential direction. For simplicity, the low-pass filters $H(z^{2^i})$, $i=0,\ldots,M-1$ that are based on the Haar filter, previously used for image low-pass filtering, were again employed. Pixel sets $c_{\rm int}$, $c_{\rm ext}$, as modified by the smoothing procedure, were then used as input to the snake, as discussed in the following section.

2.4. Active contour model

In our approach, the active contour model's energy functional given in (1) was defined as

$$E_{\rm snake} = E_{\rm cont} + E_{\rm curv} + E_{\rm image}, \qquad (5)$$

where the first two terms corresponded to the internal energy, while the third term corresponded to the external one. Specifically, $E_{\rm cont}$ was the contour continuity energy (caused the snaxels to become more equidistant), $E_{\rm curv}$ was the contour curvature energy (the smoother the contour was, the less was the curvature energy), while $E_{\rm image}$ was the image energy (forced the snake to be attracted by image features). More specifically, considering a set of snaxels $S = \{s_1, s_2, \ldots, s_N\}$ the partial energy terms were defined as

$$E_{\rm cont} = |\bar{\delta} - |s_i - s_{i-1}||, \qquad (6)$$

where $\bar{\delta}$ is the average distance between all pairs $|s_i - s_{i-1}|$,

$$E_{\rm curv} = |s_{i-1} - 2s_i + s_{i+1}|^2 \qquad (7)$$

and

$$E_{\rm image} = -|\nabla I|^2, \qquad (8)$$

where I is the image intensity.

In more detail, total energy at every point was calculated as a linear combination of the aforementioned terms, i.e.

$$E_{{\rm snake},i} = \alpha E_{{\rm cont},i} + \beta E_{{\rm curv},i} + \gamma E_{{\rm image},i}, \qquad (9)$$

where α, β and γ were appropriate weighting factors, which controlled the relative influence between the terms. In particular, α was responsible for contour continuity in that a high value made snaxels more evenly spaced, β was responsible for snake corners in that a high value for a specific snaxel made the angle between snake edges more obtuse, while γ was responsible for making snaxels more sensitive to the image energy, rather than to continuity or curvature. The parameters α, β and γ were set to 1.09, 50 and 32, respectively, on the basis of multiple experimental segmentation tests we conducted, and remained constant during the segmentation process.

2.5. In vivo validation of the segmentation model

2.5.1. In vivo IVUS dataset

To validate in vivo the proposed segmentation model, 17 arterial segments (right coronary artery, RCA, $n = 7$; left anterior descending, LAD, $n = 4$; left circumflex artery, LCx $n = 6$) with an average length of 85.7 ± 17.1 mm from 9 patients were investigated with IVUS. The Institutional Medical Ethics Committee approved the study, and all patients gave written informed consent. From the resulting pool of IVUS images, 50 were randomly selected, and segmented both manually and automatically.

2.5.2. Intra- and inter-observer agreement of manual segmentation

Manual segmentation was accomplished by two independent IVUS experts according to the accepted international standards [1], and used as reference in the method comparison study. To improve the accuracy of their segmentation, both experts were allowed to evaluate the recorded on S-VHS real-time display of IVUS images, and repeatedly edit the detected contours until full satisfaction. The intra-observer agreement (IOA) of the manual segmentation was assessed by comparing the within-expert segmentations initially and a month apart, whereas for the inter-observer agreement (INA) the between-experts segmentations compared. The IVUS morphometric parameters used for the IOA and INA of manual contour detection included lumen cross-sectional area (LCSA, mm^2), vessel cross-sectional area (VCSA, mm^2), wall cross-sectional area (WCSA, mm^2), maximum lumen diameter (MLD, mm), and maximum vessel diameter (MVD, mm), all defined in Fig. 1. The LCSA, WCSA, and MVD were used as measures for the detection accuracy of lumen borders, whereas VCSA, WCSA, and MVD were used as measures for the detection accuracy of media-adventitia borders.

2.5.3. Automated versus manual segmentation

To assess the performance of the automated segmentation versus the manual reference, the automatically determined borders compared with the ones derived from manual segmentation. Cross-sectional areas (LCSA, VCSA, and WCSA, $n = 50$) and maximum diameters (MLD and MVD, $n = 50$) were used as compared parameters. The average of these parameters in the between-experts manual segmentations was used as reference.

For the temporal evaluation of the automated method versus the manual reference, the mean duration of manual ($n = 3$) and automated segmentation ($n = 1$) were calculated and compared.

2.5.4. Statistical analysis

For the assessment of IOA and INA of manual segmentation, as well as for the method comparison study, Bland–Altman analysis [20], and linear regression analysis were applied. The analyses were performed with the statistical package SPSS 12.0 (SPSS Inc, Chicago, IL, USA). All results were expressed as mean $\pm$ SD, and $p < 0.05$ was considered as the level of significance.

3. Results

3.1. Intra- and inter-observer agreement of manual segmentation

Table 1 presents the IOA and INA of manual segmentation for all the calculated parameters. Manual segmentation had significantly high IOA and INA with mean differences (Md) very close to zero, and the differences distributed within the limits of agreement (Md$\pm$2SD). These findings supported the robustness

Table 1
Intra- and inter-observer agreement of manual segmentation

		LCSA ($n=50$)	VCSA ($n=50$)	WCSA ($n=50$)	MLD ($n=50$)	MVD ($n=50$)
IOA	r	0.99	0.99	0.99	0.98	0.99
	Md	0.13	−0.10	0.08	0.06	0.00
	±2SD	0.95	0.80	0.80	0.30	0.21
INA	r	0.96	0.98	0.97	0.95	0.96
	Md	0.40	0.10	0.30	0.16	0.06
	±2SD	2.10	1.90	2.00	0.62	0.58

IOA = Intra-observer agreement, INA = Inter-observer agreement, Md = Mean difference, ±2SD = Limits of agreement. Md and ±2SD are expressed in mm^2 for lumen cross-sectional area (LCSA), vessel cross-sectional area (VCSA), wall cross-sectional area (WCSA), and in mm for maximum luminal diameter (MLD), and maximum vessel diameter (MVD). For all r values $p<0.001$.

of the manual segmentation, utilized as reference in the subsequent method comparison study with the automated segmentation.

3.2. Automated versus manual segmentation

Bland–Altman plots of differences between automated and manual tracings against their means revealed that the proposed model had minor differences as compared with the reference manual for all the calculated parameters (Fig. 4). As shown, the mean differences (Md) for LCSA, VCSA, WCSA, MLD and MVD were $0.70 \pm 2.68\,\text{mm}^2$, $0.17 \pm 4.58\,\text{mm}^2$, $-0.53 \pm 3.50\,\text{mm}^2$, $0.15 \pm 0.56\,\text{mm}$, and $0.07 \pm 0.78\,\text{mm}$, respectively. Also, as depicted in the corresponding plots, the vast majority of differences were distributed within the limits of agreement (i.e. Md ± 2SD), suggesting a high level of agreement between manual and automated segmentation.

In addition, linear regression analysis revealed that the automated segmentation was strongly correlated with the reference manual, and yielded the following results for LCSA, VCSA, and WCSA, respectively: $y=0.78x+2.09$, $r=0.86$; $y=0.66x+3.65$, $r=0.90$; $y=0.55x+1.24$, $r=0.80$ ($p<0.0001$, $n=50$) (Fig. 5). The corresponding equations for MLD and MVD were: $y=0.78x+0.82$, $r=0.90$; $y=0.70x+1.20$, $r=0.91$ ($p<0.0001$, $n=50$). Fig. 6 depicts 12 IVUS images manually and automatically segmented. As shown, the performance of the automated segmentation was remarkably high, even in poor quality IVUS images due to artifacts, calcifications, or branches, further supporting the detection efficiency of our automated segmentation approach.

With respect to the temporal evaluation of the automated method, the required analysis time for the dataset of 50 randomly selected images reduced by 96% with our method (3.6 s per image for automated segmentation versus 85.8 s per image for manual segmentation), suggesting that apart from applicable and reliable, the method we propose is markedly rapid.

4. Discussion

In this work we present a novel method for the segmentation of IVUS images based on the coupling of a fully automated contour initialization procedure with the application of active contours. Major contributions of this work are: (a) the technique developed for automated contour initialization, confronting this way manual contour initialization which is a significant drawback in the applicability of the majority of the snake-based approaches, and (b) the in vivo assessment of the proposed segmentation approach in human coronary arteries, which revealed that our method performs highly reliable and rapid IVUS images segmentation.

4.1. Fully automated contour initialization coupling an active contour model

Traditionally, the segmentation of IVUS images was performed manually, which is a time-consuming procedure with results affected by high inter- and intra-user variability. To overcome these limitations, several approaches for semi-automated segmentation have been proposed in the literature. Sonka et al. implemented a knowledge-based graph searching method incorporating a priori knowledge on coronary artery anatomy and a selected region of interest prior to the automatic border detection [9]. Quite a few variations of active contour-based models have also been proposed [12,16,17,21]; however, the common characteristic of these approaches is that they require a varying degree of manual contour initialization prior to the application of the active contours.

However, in clinical practice the most attractive segmentation approaches are the fully automated ones. A limited number of such methods have been developed so far, such as the segmentation based on edge contrast [22]; the latter is shown to be an efficient feature for IVUS image analysis, in combination with the grey level distribution. Brusseau et al. exploited an automatic method for detecting the luminal border based on an active contour that evolves until it optimally separates regions with different statistical properties without using a pre-selected region of interest or initialization of the contour close to its final position [13]. A fuzzy clustering algorithm for adaptive segmentation of IVUS images was also investigated by Filho et al. [23], whereas Cardinal et al. presented a 3D IVUS segmentation approach, applying Rayleigh probability density functions (PDFs) for modeling the pixel grey value distribution of the vessel wall structures [24]. An automated approach based

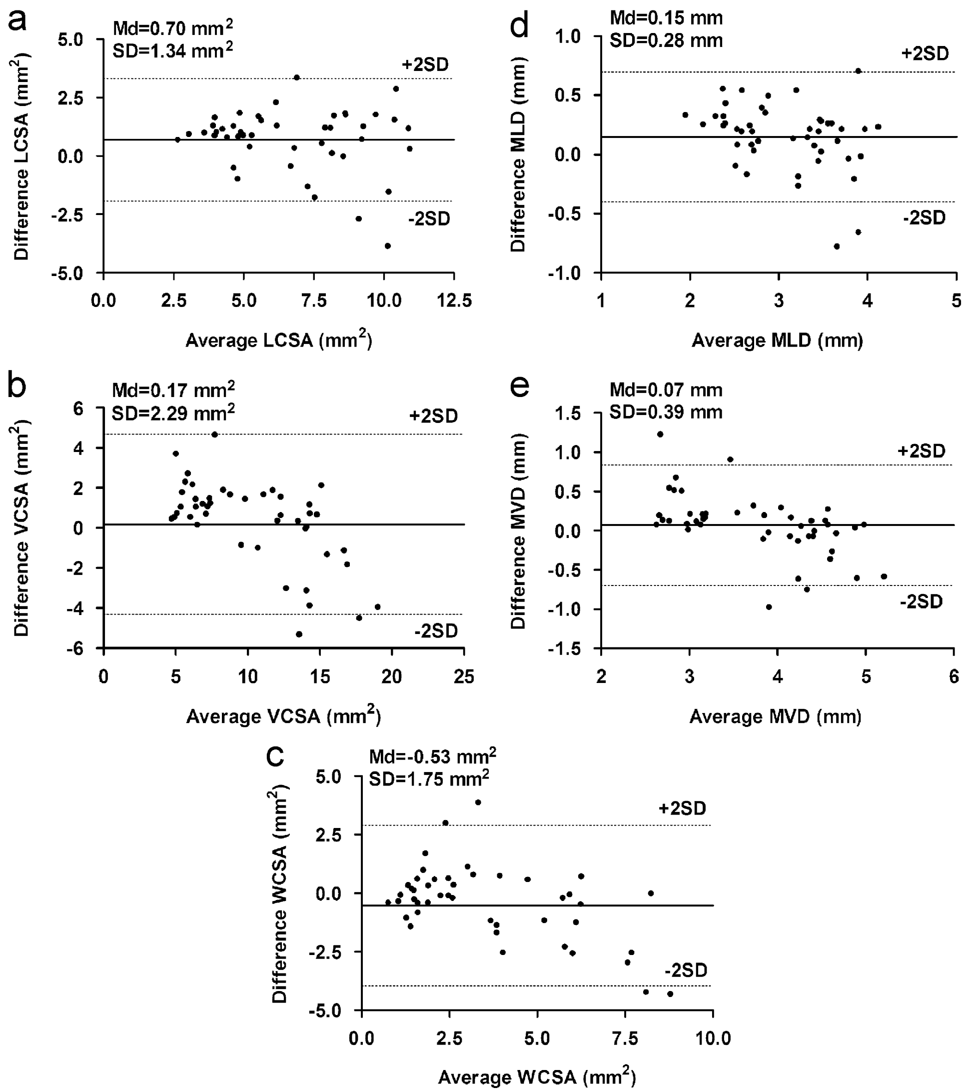

Fig. 4. Bland–Altman plots of differences between manual and automated segmentation against their mean for a, lumen cross-sectional area (LCSA, mm^2), b, vessel cross-sectional area (VCSA, mm^2), c, wall cross-sectional area (WCSA, mm^2), d, maximum luminal diameter (MLD, mm), and e, maximum vessel diameter (MVD, mm). The solid black lines represent the mean differences (Md), while the dotted lines denote the limits of agreement ($\pm$2SD).

on deformable models was also reported by Plissiti et al., who employed a Hopfield neural network for the modification and minimization of an energy function, as well as a priori vessel geometry knowledge [25].

In the current work, the active contour model developed for IVUS images segmentation was based on the OpenCV computer vision library [26]. The proposed approach did not require manual initialization of the contours; instead, the initialization of the contours in each frame was based on the analysis of IVUS morphologic characteristics. Also, the inherent property of active contours to dynamically and automatically deform added to the feasibility and accuracy of the final segmentation.

4.2. *In vivo validation of the automated segmentation method*

The proposed method was validated against manual contour detection, which was considered as the reference technique. The manual segmentation was highly reproducible and accurate in our study as indicated by the significantly high IOA and INA agreement. The validation study was performed by Bland–Altman and linear regression analysis in 50 randomly selected images, using areas and diameters as compared parameters. Bland–Altman analysis increased the reliability of the method comparison study, since it is considered as the most appropriate test for such analyses [20]. In fact, this test is considered superior to linear regression analysis given that the latter provides information about the degree of association only, ignoring the degree of agreement. Both Bland–Altman and linear regression analysis yielded considerably high agreement between the proposed and the reference method for all parameters. Also, these results were in good agreement with others reported in the literature [8,12]. As far as the analysis time is concerned, this significantly reduced by 96% in the described method as compared to the reference manual, without compromising accuracy.

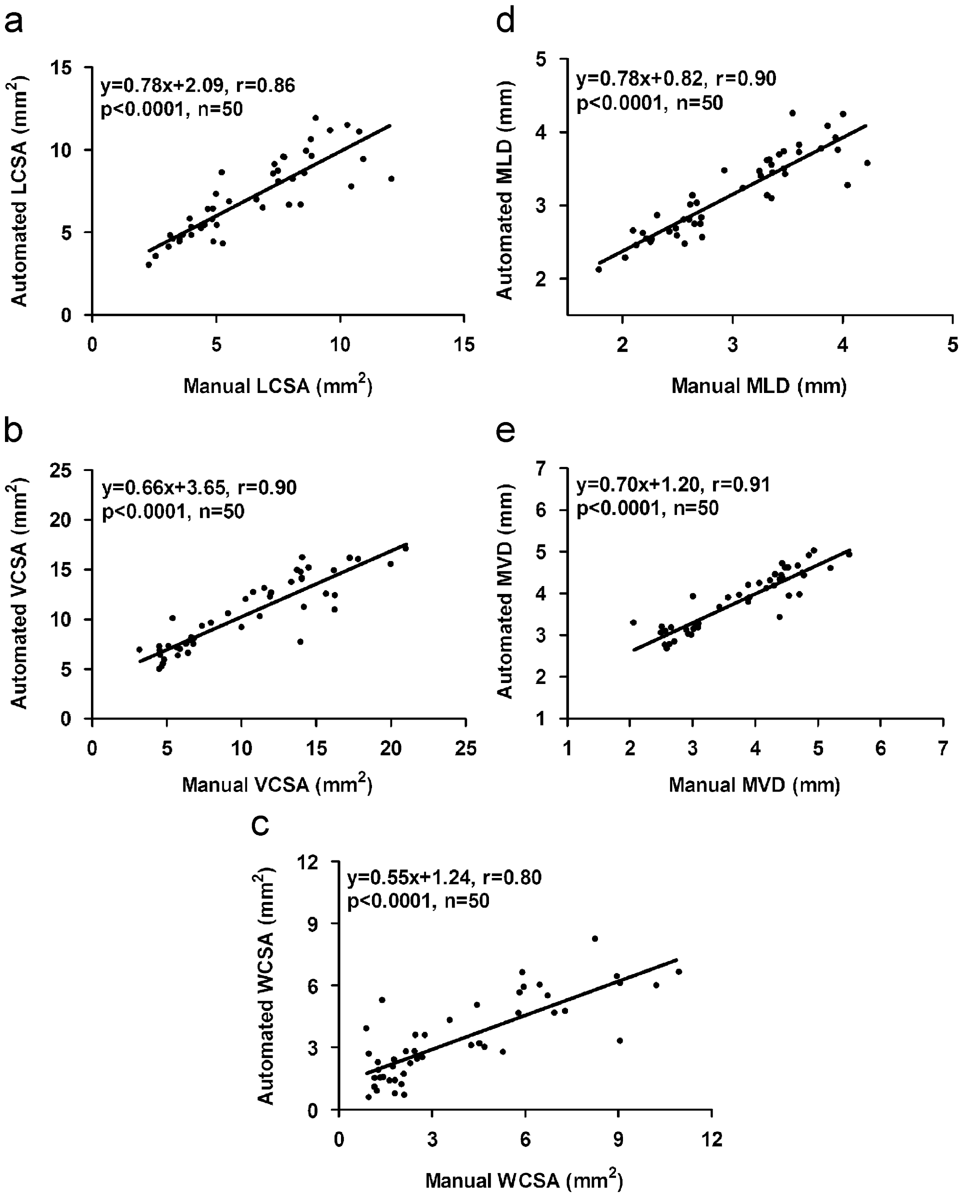

Fig. 5. Correlation between automated and manual segmentation for a, lumen cross-sectional area (LCSA, mm^2), b, vessel cross-sectional area (VCSA, mm^2), c, wall cross-sectional area (WCSA, mm^2), d, maximum luminal diameter (MLD, mm), and e, maximum vessel diameter (MVD, mm).

In addition, the constructed segmentation framework showed high effectiveness providing satisfactory border detection even in bad-quality images with either artifacts (e.g. shadowing effect of calcified areas, guidewire artifacts), or gaps due to the presence of major branches (Fig. 6).

Another asset of our methodology is that it performed very effectively in non-sequential IVUS images. This suggests that our method is quite robust, and provides the potential of combining it with other approaches that utilize the continuity of sequential IVUS frames, towards even more accurate and quicker segmentation results.

5. Conclusion and clinical perspective

The active contour-based model we present in this study constitutes a novel, fully automated and feasible approach, enabling accurate and rapid segmentation of IVUS images. Provided that the proposed approach facilitates the rapid and accurate contour detection in hundreds of IVUS images acquired during a routine pullback, it could potentially constitute a valuable tool for both clinical and research purposes. First, it could facilitate plaque morphometric analyses including planimetric, volumetric and wall thickness calculations, thereby contributing to rapid, and potentially on-site, decision-making. Similarly, the method could be utilized for the evaluation of plaque progression or regression in follow-up studies investigating the effect of drugs, or local mechanical interventions (e.g. stents).

We and others have developed and validated an in vivo IVUS and biplane angiography fusion technique for the anatomically correct 3D reconstruction of human coronary arteries [4–6,27]. This technique is coupled with computational fluid

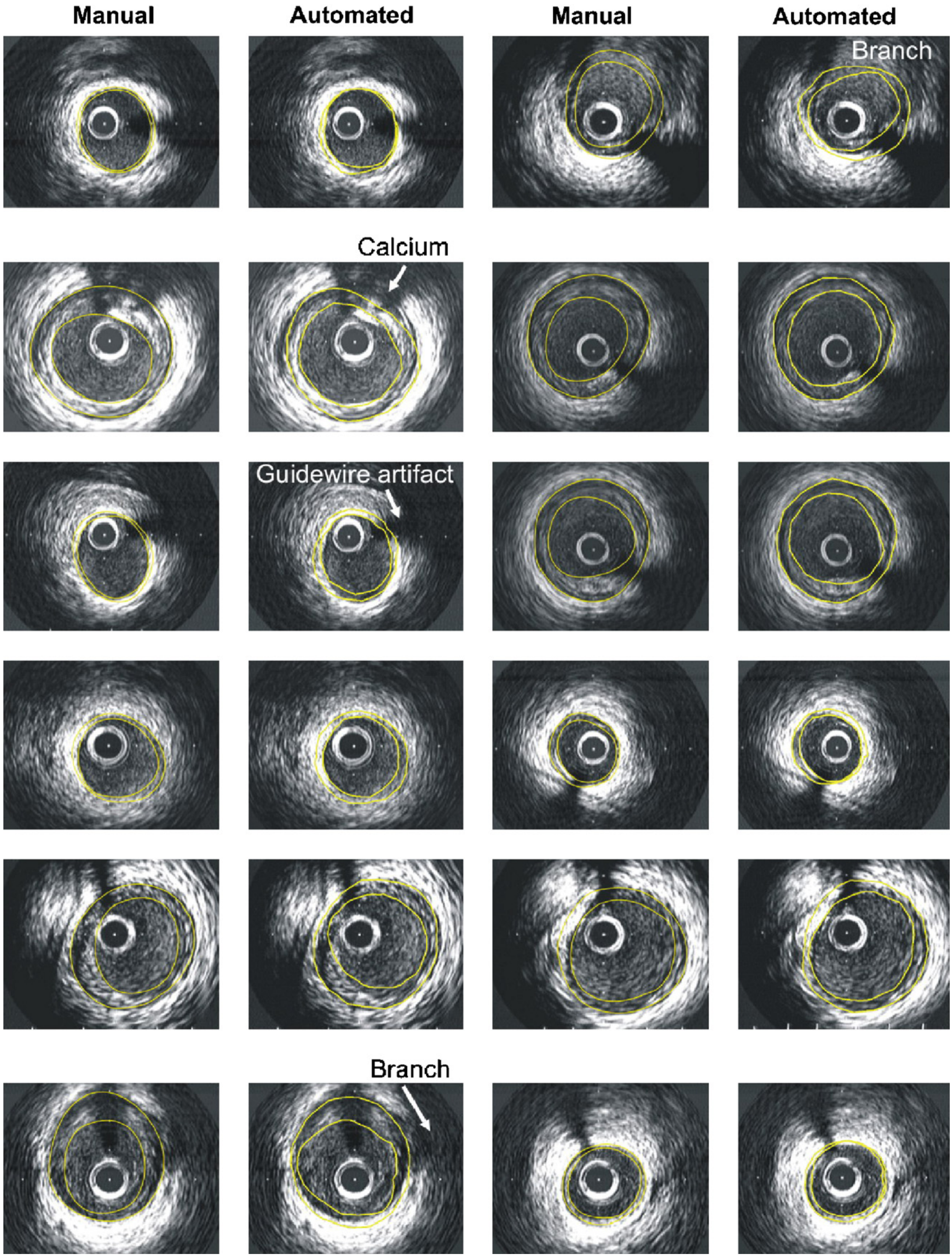

Fig. 6. A representative sample of 12 randomly selected IVUS images manually and automatically segmented. The automated segmentation performed well, even in bad-quality images with guidewire artifacts, branches, or calcifications.

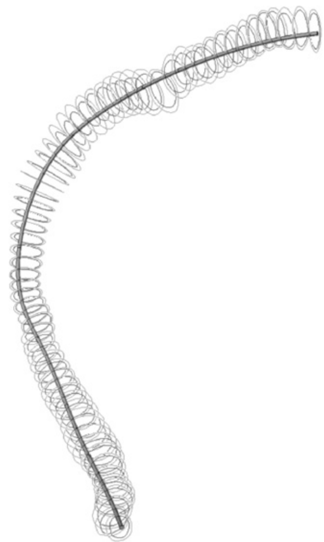

Fig. 7. An example of a 3D reconstructed right coronary artery. The cross-sections correspond to the borders extracted by applying the proposed segmentation model. The trajectory of the IVUS catheter is also depicted.

dynamics permitting the investigation of the role of local hemodynamic factors (e.g. endothelial shear stress, tensile stress) [28], and local geometric parameters (e.g. vessel curvature) [29] at certain locations along the coronary lumen, on atherosclerosis development and progression, as well as on arterial remodeling. The reliable and quick IVUS segmentation constitutes the foundation for the implementation of the abovementioned reconstruction technique, and our segmentation method provides this perspective. In Fig. 7 we present a representative example of a geometrically correct 3D reconstruction of a right coronary artery, based on the segmentation of the IVUS images with the proposed active contour model.

References

[1] G.S. Mintz, S.E. Nissen, W.D. Anderson, S.R. Bailey, R. Erbel, P.J. Fitzgerald, F.J. Pinto, K. Rosenfield, R.J. Siegel, E.M. Tuzcu, P.G. Yock, American College of Cardiology clinical expert consensus document on standards for acquisition, measurement and reporting of intravascular ultrasound studies (IVUS). A report of the American College of Cardiology task force on clinical expert consensus documents, J. Am. Coll. Cardiol. 37 (2001) 1478–1492.

[2] C. von Birgelen, E.A. de Very, G.S. Mintz, A. Nicosia, N. Bruining, W. Li, C.J. Slager, J.R. Roelandt, P.W. Serruys, P.J. deFeyter, ECG-gated three-dimensional intravascular ultrasound: feasibility and reproducibility of the automated analysis of coronary lumen and atherosclerotic plaque dimensions in humans, Circulation 96 (1997) 2944–2952.

[3] J. Klingensmith, P. Schoenhagen, A. Tajaddini, S.S. Halliburton, M. Tuzcu, S.E. Nissen, D.G. Vince, Automated three-dimensional assessment of coronary artery anatomy with intravascular ultrasound scanning, Am. Heart J. 145 (2003) 795–805.

[4] C.J. Slager, J.J. Wentzel, J.C. Schuurbiers, J.A. Oomen, J. Kloet, R. Krams, C. von Birgelen, W.J. van der Giessen, P.W. Serruys, P.J. de Feyter, True 3-dimensional reconstruction of coronary arteries in patients by fusion of angiography and IVUS (ANGUS) and its quantitative validation, Circulation 102 (2000) 511–516.

[5] A.U. Coskun, Y. Yeghiazarians, S. Kinlay, M.E. Clark, O.J. Ilegbusi, A. Wahle, M. Sonka, J.J. Popma, R.E. Kuntz, C.L. Feldman, P.H. Stone, Reproducibility of coronary lumen, plaque, and vessel wall reconstruction and of endothelial shear stress measurements in vivo in humans, Catheter Cardiovasc. Interventrons 60 (2003) 67–78.

[6] G.D. Giannoglou, Y.S. Chatzizisis, G. Sianos, D. Tsikaderis, A. Matakos, V. Koutkias, P. Diamantopoulos, N. Maglaveras, G.E. Parcharidis, G.E. Louridas, In-vivo validation of spatially correct three-dimensional reconstruction of human coronary arteries by integrating intravascular ultrasound and biplane angiography, Coron. Artery Dis. 17 (2006) 533–543.

[7] A. Mojsilovic, M. Popovic, N. Amodaj, R. Babic, M. Ostojic, Automatic segmentation of intravascular ultrasound images: a texture-based approach, Ann. Biomed. Eng. 25 (1997) 1059–1071.

[8] R. Cothren, R. Shekhar, M. Tuzcu, S. Nissen, F. Cornhill, G. Vince, Three-dimensional reconstruction of the coronary artery wall by image fusion of intravascular ultrasound and bi-plane angiography, Int. J. Card. Imaging 16 (2000) 69–85.

[9] M. Sonka, X. Zhang, M. Siebes, M. Bissing, S. DeJong, S. Collins, C. McKay, Segmentation of intravascular ultrasound images: a knowledge-based approach, IEEE Trans. Med. Imaging 14 (1995) 719–732.

[10] W. Li, W.J. Gussenhoven, J.G. Bosch, F. Mastik, J.C. Reiber, N. Bom, A computer-aided analysis system for the quantitative assessment of intravascular ultrasound images, in: Computers in Cardiology, Los Alamitos, CA, IEEE Computer Society Press, 1990, pp. 333–336.

[11] C.J. Bouma, W.J. Niessen, K.J. Zuiderveld, E.J. Gussenhoven, M.A. Viergever, Automated lumen definition from 30 MHz intravascular ultrasound images, Med. Image Anal. 1 (1997) 363–377.

[12] G. Kovalski, R. Beyar, R. Shofti, H. Azhari, Three-dimensional automatic quantitative analysis of intravascular ultrasound images, Ultrasound Med. Biol. 26 (2000) 527–537.

[13] E. Brusseau, C.L. de Korte, F. Mastik, J. Schaar, A.F. van der Steen, Fully automatic luminal contour segmentation in intracoronary ultrasound imaging-A statistical approach, IEEE Trans. Med. Imaging 23 (2004) 554–566.

[14] J.D. Klingensmith, R. Shekhar, D.G. Vince, Evaluation of three-dimensional segmentation algorithms for the identification of luminal and medial-adventitial borders in intravascular ultrasound images, IEEE Trans. Med. Imaging 19 (2000) 996–1011.

[15] M. Kass, A. Witkin, D. Terzopoulos, Snakes: active contour models, Int. J. Comp. Vis. 1 (1987) 321–331.

[16] C. Kirbas, F. Quek, A review of vessel extraction techniques and algorithms, ACM Comput. Surv. 36 (2004) 81–121.

[17] I. Kompatsiaris, D. Tzovaras, V. Koutkias, M.G. Strintzis, Deformable boundary detection of stents in angiographic images, IEEE Trans. Med. Imaging 19 (2000) 652–662.

[18] Y.S. Chatzizisis, Three-dimensional reconstruction of coronary arteries by fusion of intravascular ultrasound and biplane angiography, M.Sc. Dissertation, Aristotle University of Thessaloniki, Thessaloniki, Greece, 2004.

[19] M. Papadogiorgaki, V. Mezaris, Y.S. Chatzizisis, I. Kompatsiaris, G.D. Giannoglou, A fully automated texture-based approach for the segmentation of sequential IVUS images, 13th International Conference on Systems, Signals & Image Processing (IWSSIP 2006), Budapest, Hungary, 2006, pp. 461–464.

[20] J.M. Bland, D.G. Altman, Statistical methods for assessing agreement between two methods of clinical measurement, Lancet 1 (1986) 307–310.

[21] J.D. Klingensmith, A. Nair, et al., Segmentation of three-dimensional intravascular ultrasound images using spectral analysis and a dual active surface model, in: IEEE Ultrasonics Symposium, 2004, pp. 1765–1768.

[22] H. Zhu, Y. Liang, M.H. Friedman, IVUS image segmentation based on contrast, in: Processing of SPIE, Durham, NC, USA, 2002, pp. 1727–1733.

[23] E. dos S. Filho, M. Yoshizawa, et al., Detection of luminal contour using fuzzy clustering and mathematical morphology in intravascular ultrasound images, in: 27th Annual International Conference of the IEEE Engineering in Medicine and Biology Society, 2005, pp. 3471–3474.

[24] M.-H.R. Cardinal, J. Meunier, et al., Intravascular ultrasound image segmentation: a three-dimensional fast-marching method based on gray level distributions, IEEE Trans. Med. Imaging 25 (2006) 590–601.

[25] M.E. Plissiti, D.I. Fotiadis, L.K. Michalis, G.E. Bozios, An automated method for lumen and media-adventitia border detection in a sequence of IVUS frames, IEEE Trans. Inf. Technol. Biomed. 8 (2004) 131–141.
[26] Open Source Computer Vision Library, Intel Corp. Available at: ⟨http://sourceforge.net/projects/opencvlibrary/⟩.
[27] Y.S. Chatzizisis, G.D. Giannoglou, A. Matakos, C. Basdekidou, G. Sianos, A. Panagiotou, C. Dimakis, G.E. Parcharidis, G.E. Louridas, In-vivo accuracy of geometrically correct three-dimensional reconstruction of human coronary arteries: is it influenced by certain parameters?, Coron. Artery Dis. 17 (2006) 545–551.
[28] P.H. Stone, A.U. Coskun, S. Kinlay, M.E. Clark, M. Sonka, A. Wahle, O.J. Ilgebusi, Y. Yeghiazarians, J.J. Popma, J. Orav, R.E. Kuntz, C.L. Feldman, Effect of endothelial shear stress on the progression of coronary artery disease, vascular remodeling and in-stent restenosis in humans, Circulation 108 (2003) 438–444.
[29] R. Krams, J.J. Wentzel, J.A.F. Oomen, R. Vinke, J.C.H. Schuurbiers, P.J. de Feyter, P.W. Serruys, C.J. Slager, Evaluation of endothelial shear stress and 3D geometry as factors determining the development of atherosclerosis and remodeling in human coronary arteries in-vivo: combining 3D reconstruction from angiography and IVUS (ANGUS) with computational fluid dynamics, Arterioscler. Thromb. Vasc. Biol. 17 (1997) 2061–2065.

George D. Giannoglou was born in Edessa, Greece, in 1947. He received the M.D. degree from the Medical School, Aristotle University of Thessaloniki, Greece, in 1971 and the Ph.D. degree in 1985. Since 1990, he has been with the Medical School, Aristotle University of Thessaloniki, Greece, where he is the Associate Professor in Cardiology. His research interests focus on atherosclerosis and biomedical engineering.

Yiannis S. Chatzizisis was born in Larisa, Greece, in 1976. He received the M.D. degree from the Medical School, Aristotle University of Thessaloniki (A.U.Th), Thessaloniki, Greece, in 2000, and the M.Sc. degree from the same university in 2004. Since 2004, he is a Ph.D. candidate in A.U.Th with funding from the Greek State Scholarships Foundation. In 2005, he completed the residency in Internal Medicine at the AHEPA University Hospital, Thessaloniki, Greece. Since 2000, he has been a Research Fellow in Cardiology at the Cardiovascular Engineering and Atherosclerosis Laboratory, A.U.Th.. Since 2005 he has been Research Fellow in Cardiology at the Brigham and Women's Hospital, Harvard Medical School and the Massachusetts Institute of Technology. His research interests include molecular biology of atherosclerosis, cardiovascular fluid dynamics, and cardiovascular imaging.

Vassilis Koutkias was born in Lamia, Greece, in 1975. He received the Diploma in Electrical & Computer Engineering (1998) and the M.Sc. (2001) and Ph.D. (2005) in Medical Informatics all from the Aristotle University of Thessaloniki (A.U.Th.), Greece. Currently, he works as a Research Associate at the Lab of Medical Informatics, A.U.Th. His research interests include multiagent systems applied in healthcare and bioinformatics, grid technologies, telemedicine systems, pervasive healthcare, as well as medical imaging. He has been involved in several R&D projects in the e-health sector and he is part-time lecturing at A.U.Th. and at the Technological Educational Institute of Thessaloniki. Dr. Koutkias is member of the IEEE and the Technical Chamber of Greece.

Ioannis Kompatsiaris received the Diploma degree in electrical engineering and the Ph.D. degree in 3D model based image sequence coding from the Aristotle University of Thessaloniki (A.U.Th.), Thessaloniki, Greece, in 1996 and 2001, respectively. He is a Senior Researcher (Researcher C') with the Informatics and Telematics Institute and currently he is leading the Multimedia Knowledge Group. His research interests include semantic annotation of multimedia content, multimedia information retrieval and knowledge discovery, medical imaging, and MPEG-4 and MPEG-7 standards. He is the coauthor of six book chapters, 17 papers in refereed journals and more than 60 papers in international conferences. He is a member of IEEE and of the IEE VIE TAP.

Maria Papadogiorgaki was born in Chania, Crete Island, Greece, in 1977. She received the Diploma degree in Electrical and Computer Engineering and the M.Sc. degree in Medical Informatics from the Aristotle University of Thessaloniki, Thessaloniki, Greece, in 2003, and 2006, respectively. Since 2003, she is a Research Assistant with the Informatics and Telematics Institute/Centre for Research and Technology Hellas, Thessaloniki, Greece. Her research interests include medical image analysis/processing, machine learning and personalization systems. She is a member of the Technical Chamber of Greece.

Vasileios Mezaris received the Diploma degree and Ph.D. in Electrical and Computer Engineering from the Aristotle University of Thessaloniki, Thessaloniki, Greece, in 2001 and 2005, respectively. He is a postdoctoral research fellow with the Informatics and Telematics Institute/Centre for Research and Technology Hellas, Thessaloniki, Greece. His research interests include still image segmentation, video segmentation and object tracking, multimedia standards, knowledge-assisted multimedia analysis, medical image analysis, knowledge extraction from multimedia, content-based and semantic indexing and retrieval. He is a member of the IEEE and the Technical Chamber of Greece.

Eirini Parissi was born in Thessaloniki, Greece in 1982. She received the Diploma degree in Electrical Engineering from the Aristotle University of Thessaloniki. She is a Research Assistant in CERTH/ITI since 2005. Her research interests include medical image processing, ontology engineering and semantic reasoning applications on medical information and risk prediction systems.

Panagiotis Diamantopoulos was born in Athens, Greece, in 1973. He received a B.Eng. (Hons.) Degree in Mechanical Engineering in 1995, University of Brighton and a D.Phil. in Biomedical Engineering in 2001, University of Sussex. He is the Director of the Biomedical Modeling Unit (BioModel) in the School of Science & Technology at the University of Sussex, UK. He has many years experience on human modeling techniques and has extensively investigated the integration of Medical Imaging with Computer Aided Design, Finite Element Analysis and Rapid Manufacturing methods. He has contributed to over 100 international conferences on the topic and has organized relevant workshops and meetings. Among other professional affiliations, he is a member of the European Society of Biomechanics, the International Society of Biomechanics and the International Society of Computer Assisted Surgery.

Michael Gerassimos Strintzis received the Diploma degree in electrical engineering from the National Technical University of Athens, Athens, Greece, in 1967, and the M.A. and Ph.D. degrees in electrical engineering from Princeton University, Princeton, NJ, in 1969 and 1970, respectively. He then joined the Electrical Engineering Department at the University of Pittsburgh, Pittsburgh, PA, where he served as Assistant Professor (1970–1976) and Associate Professor (1976–1980). Since 1980, he has been Professor of electrical and computer engineering at the University of Thessaloniki, Thessaloniki, Greece, and, since 1999, Director of the Informatics and Telematics Research Institute, Thessaloniki. His current research interests include 2D and 3D image coding, image processing, biomedical signal and image processing, and DVD and Internet data authentication and copy protection. In 1984, Dr. Strintzis was awarded one of the Centennial Medals of the IEEE. He is a Fellow of the IEEE.

Nicos Maglaveras received the Diploma in Electrical Engineering from the Aristotle University of Thessaloniki (A.U.Th.), Greece, in 1982, and the M.Sc. and Ph.D. degrees from Northwestern University, Evanston, IL, in 1985 and 1988, respectively, in Electrical Engineering with emphasis in Biomedical Engineering. He is currently the Associate Professor in the Lab of Medical Informatics, A.U.Th. His current research interests include non-linear biological systems simulation, cardiac electrophysiology, medical expert systems, ECG analysis, medical imaging and neural networks. He has published more than 100 papers in refereed international journals and conference proceedings. He has developed graduate and undergraduate courses in the areas of medical informatics, biomedical signal processing and biological systems simulation. He has served as a reviewer in CEC AIM technical reviews and in a number of international journals, and participated as coordinator or core partner in national and CEC-funded research projects. Dr. Maglaveras is a senior member of the IEEE and member of the Greek Technical Chamber, the New York Academy of Sciences, CEN/TC251 and Eta Kappa Nu.

George E. Parcharidis is Director of the First Cardiology Department, AHEPA University General Hospital, Aristotle University of Thessaloniki and also Chairman of the Greek College of Cardiology. He has participated in numerous Greek and international scientific meetings. He has published 50 papers indexed in Medline.

George E. Louridas was born in Thessaloniki, Greece. He received the M.D. degree from the Medical School, Aristotle University of Thessaloniki, Greece, in 1964 and the Ph.D. degree in 1973. Since 1988, he was a Professor in Cardiology and since 2006 he is a Professor Emeritus.